Title

Comprehensive Mutagenesis of Herpes Simplex Virus 1 Genome Identifies UL42 as an Inhibitor of Type I Interferon Induction.

Journal

Journal of Virology, 93(23)

ISSN

0022-538X

Authors

Chapon, Maxime
Parvatiyar, Kislay
Aliyari, Saba Roghiyh
et al.

Publication Date

2019-12-01

DOI

10.1128/jvi.01446-19

Peer reviewed

AMERICAN SOCIETY FOR MICROBIOLOGY | Journal of Virology®

PATHOGENESIS AND IMMUNITY

Comprehensive Mutagenesis of Herpes Simplex Virus 1 Genome Identifies UL42 as an Inhibitor of Type I Interferon Induction

Maxime Chapon,[a] Kislay Parvatiyar,[a]* Saba Roghiyh Aliyari,[a] Jeffrey S. Zhao,[a] Genhong Cheng[a]

[a]Department of Microbiology, Immunology, and Molecular Genetics, University of California, Los Angeles, Los Angeles, California, USA

ABSTRACT In spite of several decades of research focused on understanding the biology of human herpes simplex virus 1 (HSV-1), no tool has been developed to study its genome in a high-throughput fashion. Here, we describe the creation of a transposon insertion mutant library of the HSV-1 genome. Using this tool, we aimed to identify novel viral regulators of type I interferon (IFN-I). HSV-1 evades the host immune system by encoding viral proteins that inhibit the type I interferon response. Applying differential selective pressure, we identified the three strongest viral IFN-I regulators in HSV-1. We report that the viral polymerase processivity factor UL42 interacts with the host transcription factor IFN regulatory factor 3 (IRF-3), inhibiting its phosphorylation and downstream beta interferon (IFN-β) gene transcription. This study represents a proof of concept for the use of high-throughput screening of the HSV-1 genome in investigating viral biology and offers new targets both for antiviral therapy and for oncolytic vector design.

IMPORTANCE This work is the first to report the use of a high-throughput mutagenesis method to study the genome of HSV-1. We report three novel viral proteins potentially involved in regulating the host type I interferon response. We describe a novel mechanism by which the viral protein UL42 is able to suppress the production of beta interferon. The tool we introduce in this study can be used to study the HSV-1 genome in great detail to better understand viral gene functions.

KEYWORDS HSV-1, IRF-3, UL42, interferon

Herpes simplex virus 1 (HSV-1) is the most common *Alphaherpesvirinae* virus infecting humans, with up to 90% of the population infected depending on age and location (1). It is transmitted by contact and infects epithelial cells before migrating through neuronal axons to the nearest sensory neuron nucleus, where it usually goes into a state of latency (2). Viral reactivation typically takes place after intervals of several months and generally does not lead to complications in immunocompetent individuals. As a common pathogen, HSV-1 has been the focus of years of investigation into its biology (reviewed in reference 3). HSV-1 is composed of an ~152-kbp double-stranded DNA genome that contains over 80 open reading frames (ORFs). Many encode proteins that have been identified to antagonize or modulate innate host defense programs to evade immune detection and optimize viral survival (reviewed in references 4 and 5).

The induction of type I interferon (IFN-I) is an essential component of the innate antiviral immune response, culminating in the inhibition of viral replication and dissemination (6). Cells detect the presence of pathogen-associated molecular patterns (PAMPs) through interaction with germ line-encoded pattern recognition receptors (PRRs), where receptor ligation leads to the induction of proinflammatory and IFN-I cytokines via the nuclear factor NF-κB and IFN regulatory factor 3 (IRF-3) transcription factors, respectively (7). For instance, detection of viral DNA in the cytosolic compartment via the cyclic GMP-AMP (cGAMP) synthase (cGAS) PRR yields the production of the second messenger cGAMP, which activates the downstream adaptor molecule stimu-

Citation Chapon M, Parvatiyar K, Aliyari SR, Zhao JS, Cheng G. 2019. Comprehensive mutagenesis of herpes simplex virus 1 genome identifies UL42 as an inhibitor of type I interferon induction. J Virol 93:e01446-19. https://doi.org/10.1128/JVI.01446-19.

Editor Jae U. Jung, University of Southern California

Address correspondence to Genhong Cheng, gcheng@mednet.ucla.edu.

* Present address: Kislay Parvatiyar, Department of Microbiology and Immunology, Tulane University School of Medicine, New Orleans, Louisiana, USA

Received 26 August 2019
Accepted 2 September 2019
Accepted manuscript posted online 11 September 2019
Published 13 November 2019

lator of interferon genes (STING) (8, 9). Signal bifurcation at the level of STING results in NF-κB and IRF-3 activation via tumor necrosis factor (TNF) receptor-associated factor 6 (TRAF6) and TANK-binding kinase 1 (TBK1), respectively (10). Activated IRF-3 translocates to the nucleus, where it stimulates the transcription of IFN-I genes, such as beta interferon (IFN-β). IFN-I production and signaling lead to transcriptional changes in an autocrine and paracrine manner through binding to its receptor IFN-α/β receptor (IFNAR). IFNAR signals through a Janus kinase/signal transducers and activators of transcription (JAK/STAT) pathway and leads to the activation of interferon-stimulated response element (ISRE)-controlled genes. These products include some 300 factors that collectively foster an antiviral state (reviewed in reference 6). To overcome host barriers, viruses have evolved means to suppress the IFN-I response, whether by blocking interferon production, downstream signaling, or specific interferon-stimulated genes (ISGs) (reviewed in references 11 and 12). Indeed, several HSV-1 proteins are known to directly target different components of the IFN-I signaling pathway, such as cGAS, STING, TBK1, and IRF-3 (13–16).

To date, most of the investigation into HSV-1 biology has been carried out by creating viral strains lacking a specific ORF. While highly successful, this method can present disadvantages, such as labor intensiveness, the difficulty in assessing multifunctional proteins, and a lack of insight into intergenic regions. We therefore chose to use a method that has proven successful in the study of other viral (17–19) and bacterial (20, 21) genomes. We created an HSV-1 mutant library by random insertion of a disruptive 1.2-kbp transposon across the viral genome. We then subjected the viral library to serial passaging in the presence or absence of type I interferon selective pressure to identify novel IFN-I-regulating viral proteins. We found that one of the major such regulatory proteins is the viral DNA polymerase processivity factor UL42. We report that UL42 is able to target IRF-3, prevent its phosphorylation, and prevent IFN-β transcriptional induction. Our study introduces a new tool to study the HSV-1 genome and identifies a novel mechanism by which this virus is able to prevent IFN-I activation.

RESULTS

Generation of a comprehensive HSV-1 mutant library. Herpes simplex viruses have undergone extensive studies where viral gene functional analyses have largely been accomplished through targeted mutations. A drawback of this approach is the difficulty in assessing the relative strengths of two mutants sharing a similar phenotype. In order to interrogate the viral genome in an unbiased fashion, we generated a viral mutant library. We modified a MuA-based transposon system by inserting a BpuEI type IIS restriction enzyme site at the final nucleotide of the inverted terminal repeat. The BpUEI enzyme cleaves 16 nucleotides downstream from its restriction site, providing us with the ability to sequence 16 nucleotides on each end of the transposon insertion site (Fig. 1A and Materials and Methods). We then used the MuA transposase to randomly insert the 1.2-kb transposon into a bacterial artificial chromosome containing the HSV-1 genome (BAC HSV-1) (Fig. 1A). We transformed the library into *Escherichia coli* cells and collected around 8,000 independent clones as determined by sequencing, generating a mutant library with an average of one insertion for every 20 bp. As expected, no clones with an insertion in the BAC maintenance genes were isolated, as these clones are unable to maintain replication in *E. coli* (Fig. 1B). Regions containing short repeats, while covered by the BAC library, do not provide enough diversity to align to the reference genome with sufficient confidence and are therefore excluded from our analysis. Alignment of the library to our wild-type reference genome (GenBank accession number MN458559) consistently exceeded 90% of the processed reads (workflow is described in Materials and Methods).

Library selection in wild-type cells reveals relative dispensability of unique short (US) genes. We transfected the BAC HSV-1 library into human embryonic kidney 293T (HEK293T) cells and expanded the viruses in African green monkey kidney (Vero) cells to generate our input viral library. During library selection *in vitro*, reduced transposon coverage in a specific gene is most likely the result of a loss of viral fitness

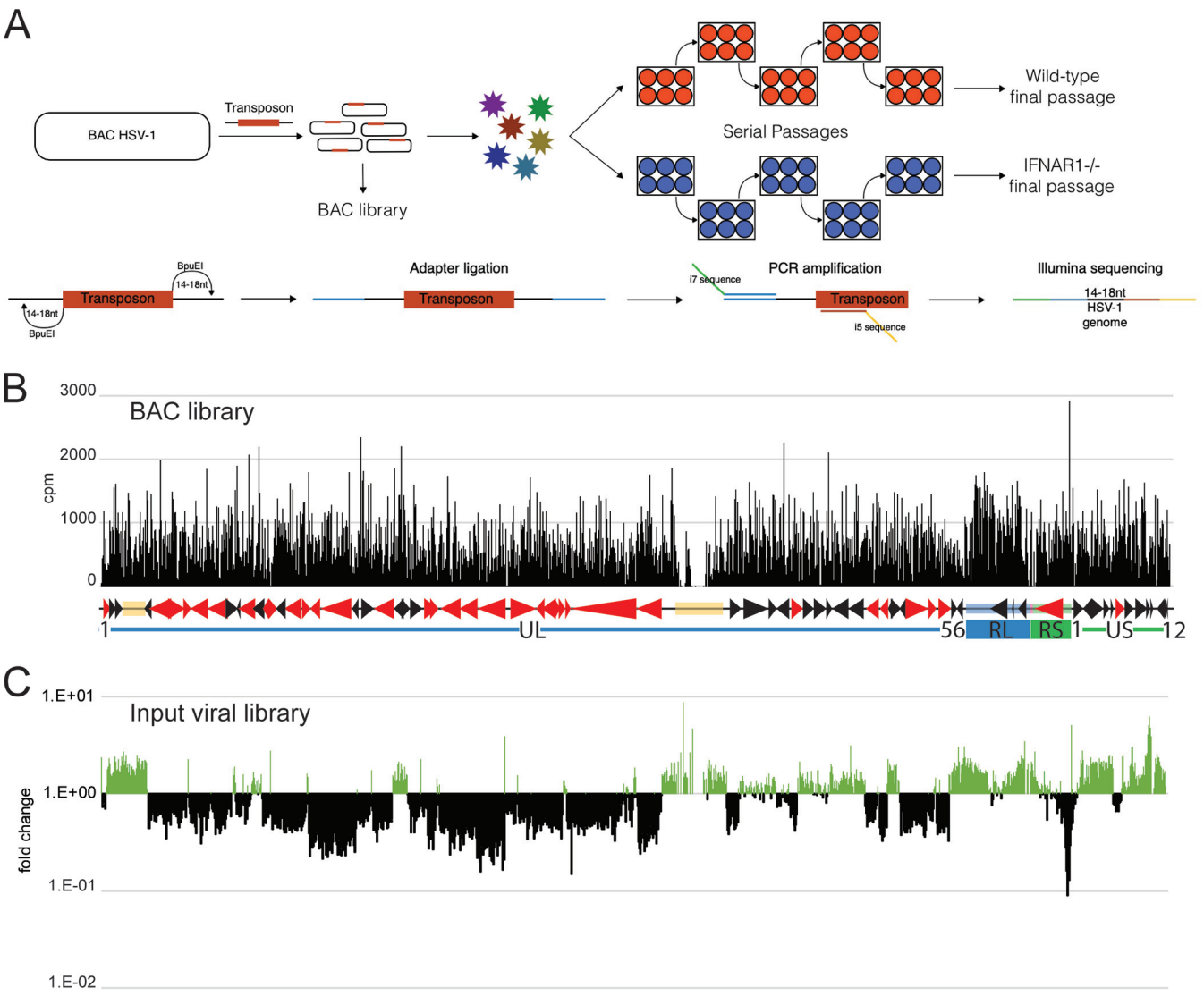

FIG 1 Construction of a comprehensive HSV-1 mutant library. (A) Top, a 1.2-kb transposon containing BpuEI type IIS restriction enzyme sites at each end was randomly inserted into a bacterial artificial chromosome (BAC) containing the entire HSV-1 genome. The BAC library was amplified in *E. coli* cells, and ~8,000 clones were isolated. It was then transfected into HEK293T cells. The viral library was expanded in Vero cells and serially passaged in different cell types. The viral mutants were collected, the transposon insertion sites sequenced, and their relative amounts were compared to the amounts of the corresponding sites in the BAC library to determine viral fitness. Bottom, viral DNA was digested with BpuEI, cutting 16 nt into the genome surrounding the transposon. Adapters were enzymatically ligated, and barcodes added by PCR. (B) BAC mutant library coverage. Yellow boxes represent BAC and reporter cassettes unrelated to the viral life cycle. Black arrows represent nonessential viral genes, while red arrows represent essential viral genes (46). The blue and green boxes represent the long and short terminal repeats, respectively. Each bar represents a 100-bp window of the viral genome. (C) Fold changes between the BAC library and the first-generation viral library as determined by TnSeqDiff.

caused by disruption of said gene by transposon insertion. These genes are therefore candidates for further analysis, as they are potentially important for viral survival. By comparing the BAC HSV-1 library to the input library, we noticed that the strongest loss of transposon coverage occurred at the viral origin of replication OriS, located in the repeat short fragment (Fig. 1C). This was expected, as targeted sequencing of the wild-type (WT) BAC HSV-1 revealed it to be most closely related to the ZW6 strain (GenBank accession number KX424525.1), with the addition of the BAC and firefly luciferase reporter cassettes and a deletion of the OriL origin of replication. Indeed, while WT HSV-1 can replicate with a single origin of replication (22), a mutant with a deletion of OriS in an OriL-deficient strain is not viable, explaining the disappearance of these mutants.

In order to generate a comprehensive map of essential genes of HSV-1 and confirm the validity of our screening method, we subjected the library to five consecutive

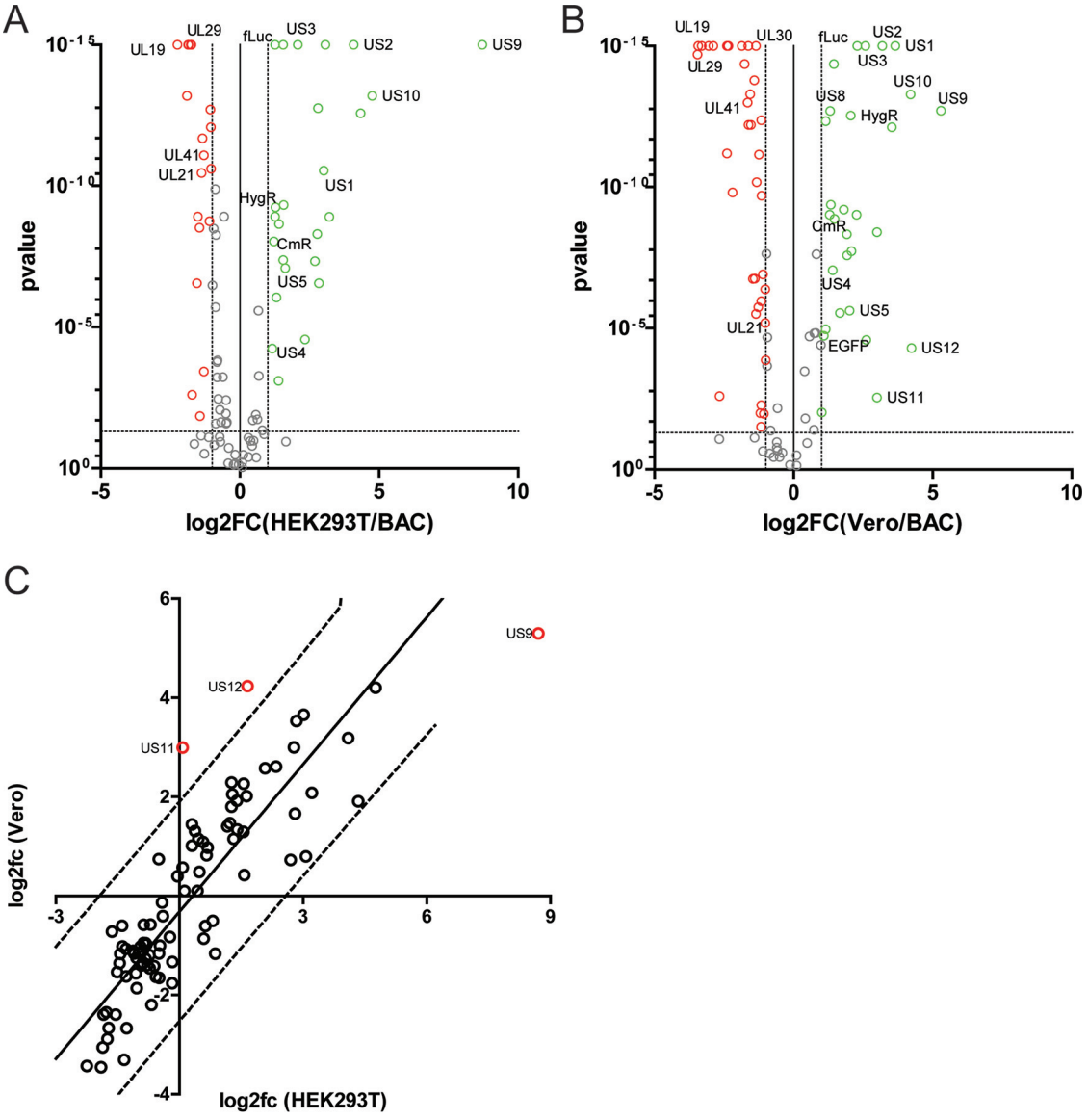

FIG 2 Library selection in wild-type cells reveals relative dispensability of unique short genes. (A, B) HEK293T or Vero cells were infected with the viral library in triplicate for five serial passages. Each triplicate was kept independent from the others during all passages. After 5 passages, the surviving mutants were identified by sequencing and their abundances were compared to the original bacterial artificial chromosome (BAC) library using TnSeqDiff. (A) Log_2 fold change (log2FC) in abundance between the BAC library and the final passage in HEK293T cells. (B) Log_2 fold change in abundance between the BAC library and the final passage in Vero cells. (C) Comparison of the log_2 fold changes from the BAC library to final passage between HEK293T (*x* axis) and Vero cells (*y* axis). Linear regression and 95% prediction intervals are shown. Fold changes and *P* values were calculated using TnSeqDiff (23).

rounds of selection in WT cell lines. The trend initiated in the first generation of virus was confirmed after five successive passages in either Vero cells or HEK293T cells (Fig. 2A and B). As expected, we saw reductions in the relative levels of coverage between the BAC library and the final-passage viral libraries for most genes that have previously been reported as essential for viral growth. In this experimental setup, different mutants are competing with each other such that the fastest growing, or fittest, will increase in proportion during passaging. Interestingly, viruses with insertions in genes encoding proteins unrelated to the viral life cycle (i.e., green fluorescent protein, firefly luciferase, chloramphenicol resistance, and hygromycin B resistance) were not the fittest under these *in vitro* conditions. In contrast, viruses with transposon insertions in the terminal repeats or the unique short (US) sequences (except US6) grew better, as

shown by the results in Fig. 1C, where most of the positive fold changes are shifted to the right end of the genome.

We also found that several nonessential genes were necessary for proper fitness. For example, insertions in genes like UL21 and UL41 were deleterious to relative mutant abundance (Fig. 2A and B). Only three genes were differentially selected between Vero and HEK293T cells: US9, US11, and US12 (Fig. 2C). US11 and US12 disruption was better supported in Vero cells than in HEK293T cells. US9 was nonessential in both cell types, and clones in which US9 was disrupted were particularly successful in HEK293T cells.

Library selection in WT versus IFNAR1$^{-/-}$ A549 cells reveals strong immunomodulatory candidates. To investigate how HSV-1 suppresses the IFN-I response, we passaged the viral library in WT or IFNAR1$^{-/-}$ A549 cells (Fig. 3A and B, respectively). We then compared the selective pressures in the two different cell lines, looking for genes that were nonessential in IFNAR1$^{-/-}$ cells but negatively selected in WT cells. We used TnSeqDiff to calculate the respective enrichment for each open reading frame of HSV-1 (Fig. 3C) (23). Importantly, intact viruses, which contained transposon insertions in genes not related to HSV-1 biology (Fig. 3C, green dots), did not show differential growth between the WT and IFNAR1$^{-/-}$ cell lines. Most gene mutations biased the viruses bearing them toward better growth in IFNAR1$^{-/-}$ cells, which is consistent with a reduced selective pressure. Some mutants containing insertions targeting known regulators of IFN-I production (UL24, VP16, ICP27/UL54, UL36, and UL37) were unable to grow in IFNAR1$^{-/-}$ cells. All these mutants, apart from those in which UL24 was disrupted, were very strongly selected in WT cells ($\log_2$ fold change lower than -5). ICP0 mutants showed a trend toward better growth in IFNAR$^{-/-}$ cells. Mutants with mutations in proteins that alter interferon production (US3 and VP24) or its downstream effectors (ICP34.5) were biased toward better growth in IFNAR1$^{-/-}$ but did not show the strongest phenotype (24–26). Indeed, the three genes whose mutation led to the most strongly biased growth in IFNAR1$^{-/-}$ cells—US1, UL42, and UL44—have not previously been described to inhibit interferon activity in HSV-1 infection.

To determine whether the three candidate proteins acted directly on IFN-β transcriptional activation, we overexpressed these genes in a cell line expressing an IFN-β luciferase reporter. We found that the expression of US1 and UL42, but not UL44, inhibited STING-dependent IFN-β activation (Fig. 3D). Because UL42 showed the strongest phenotype, we investigated its mechanism of action further.

UL42 inhibits interferon beta production and interacts with IRF-3. Further characterization of UL42 indicated a dramatic effect on the IFN-I response, as UL42 overexpression was sufficient to block IFN-β–luciferase reporter activity induced by overexpression of STING, TBK1, or IRF-3 (Fig. 4A to C). B-DNA transfection recapitulates the cellular response to cytoplasmic DNA of foreign origin, causing cGAS activation and the production of cyclic dinucleotide second messengers that activate the STING/TBK1/IRF-3 pathway. Following B-DNA stimulation, UL42 was able to suppress transcriptional activation of IFN-β and of its downstream interferon-stimulated gene (ISG) ISG54 (Fig. 4D and E) similarly to A20, an inhibitor of TBK1-mediated activation of IRF-3 (27).

As IRF-3 overexpression could not recapitulate IFN-β–luciferase activation (Fig. 4C), we hypothesized that UL42 inhibits IFN-β by regulating IRF-3 function. Using coimmunoprecipitation, we found that UL42 interacts with IRF-3 (Fig. 4F). The interferon enhanceosome is composed of four binding sites for three transcription factors: NF-κB, IRFs, and AP-1. Zhang et al. previously reported the ability of UL42 to inhibit tumor necrosis factor alpha (TNF-α)-stimulated NF-κB activation (28). We were able to confirm this result using an NF-κB–luciferase reporter and TRAF6 overexpression (Fig. 4G). Having established that UL42 can act on NF-κB and IRF-3, we undertook to check whether it could also inhibit AP-1 activation, using a luciferase reporter. Under phorbol myristate acetate (PMA) stimulation, we found that UL42 overexpression did not prevent AP-1 activation (Fig. 4H). To further confirm the specificity of inhibition, we showed that UL42 overexpression does not suppress forskolin-induced activation of the cyclic AMP (cAMP) response element (CRE) (Fig. 4I).

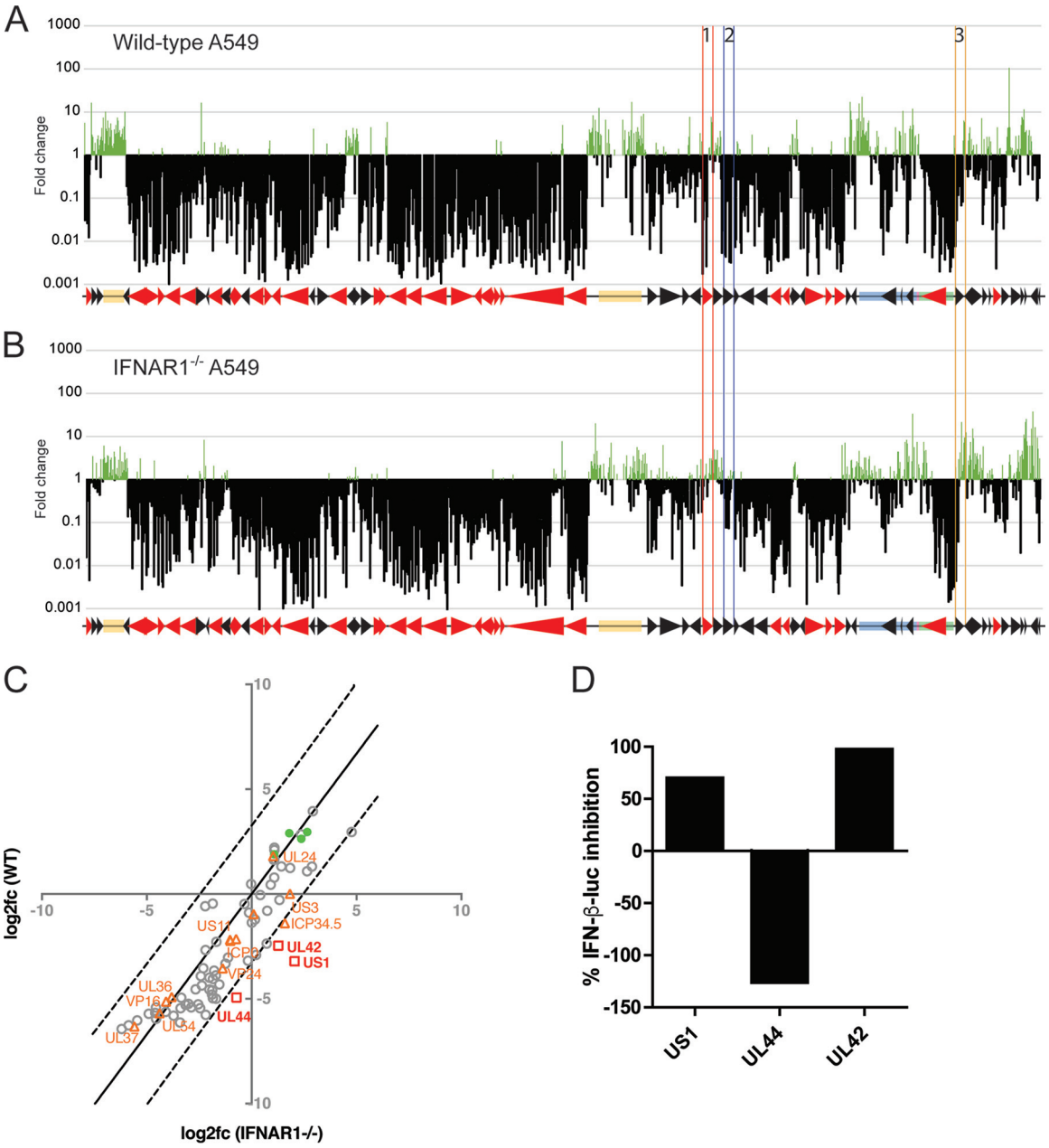

FIG 3 Differential viral library selection with or without type I interferon pressure reveals novel immunomodulatory candidates. (A) Fold changes between BAC library and final passage in wild-type A549 cells. Genes marked 1, 2, and 3 indicate UL42, UL44, and US1, respectively. (B) Fold changes between BAC library and final passage in IFNAR1$^{-/-}$ A549 cells. (A and B) Colored arrows and boxes are described in the legend to Fig. 1B. (C) Comparison of the $\log_2$ fold changes in WT (*y* axis) and IFNAR1$^{-/-}$ (*x* axis) A549 cells. Green dots represent transposon insertions in genes not related to the viral life cycle, i.e., intact virus. Orange triangles represent genes previously identified as viral regulators of the IFN-I response. Red squares highlight novel immunomodulatory candidates. Linear regression through the origin and 95% prediction bands are shown. Fold changes were calculated using TnSeqDiff. (D) HEK293T cells were cotransfected with an IFN-β–luciferase reporter and vector control or UL42, UL44, or US1 with or without STING. Sixteen hours later, the cells were lysed and luciferase activity was measured. Fold activation was determined by dividing the reporter activity with STING by that without STING. Inhibition was calculated by subtracting the fold activation with UL42, UL44, or US1 from the fold activation with empty vector control. Percent inhibition was calculated by dividing the inhibition by the fold activation with empty vector control.

UL42 mutant lacking interaction with IRF-3 fails to impair IFN-β activation. UL42 is a DNA polymerase processivity factor that binds DNA via an extensive positively charged patch on its surface (Fig. 5A) (29). Arginine-to-alanine mutations on this surface disrupt UL42's binding to DNA, inhibiting its polymerase processivity factor activity (30). Notably, mutations in this domain also reduced UL42-mediated inhibition of NF-κB

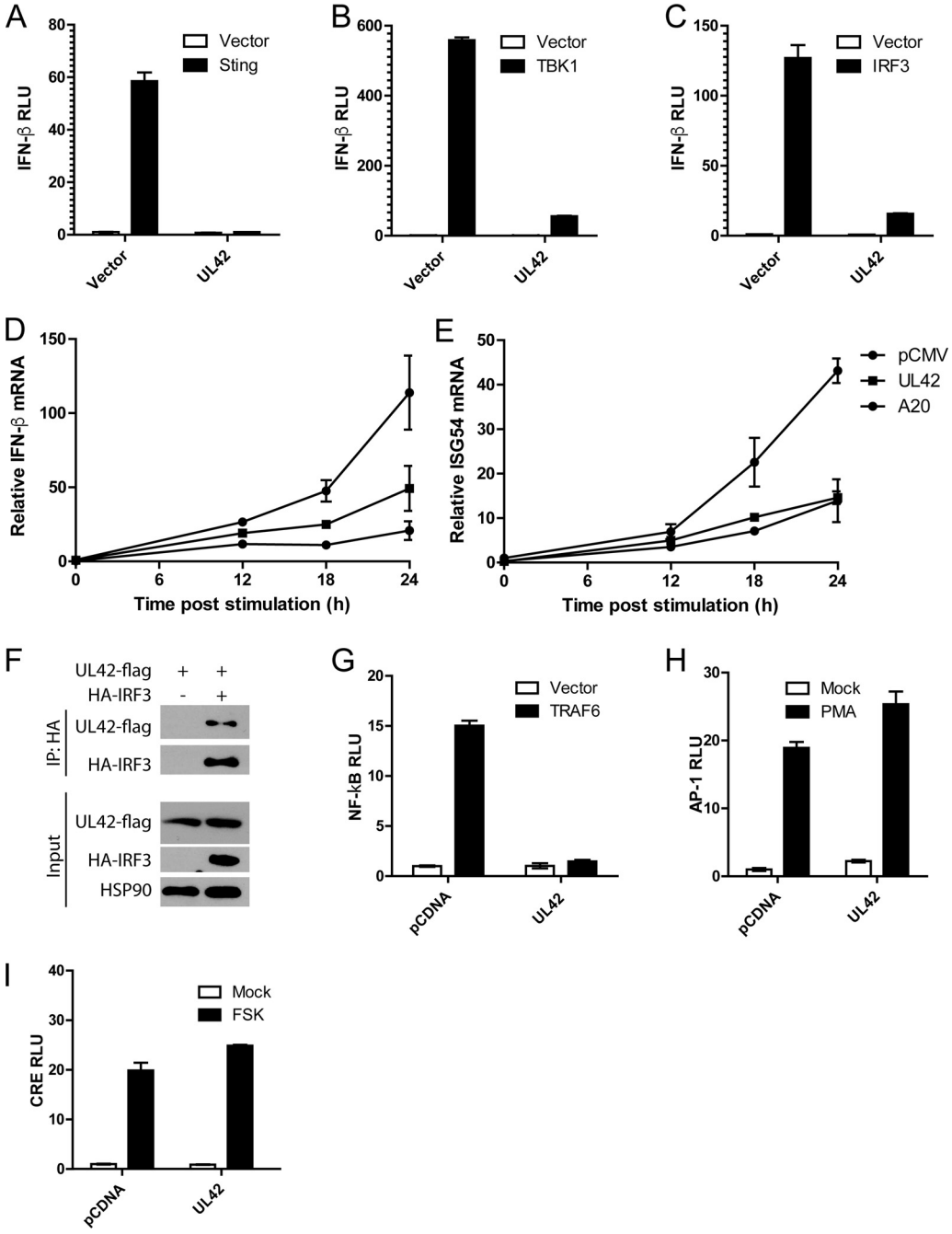

FIG 4 UL42 specifically inhibits IFN-β transcriptional activation and interacts with IRF-3. (A to C) HEK293T cells were cotransfected with an IFN-β–luciferase reporter or UL42-Flag or vector control and STING (A), TBK1 (B), or IRF-3 (C). Sixteen hours after transfection, luciferase activity was measured. (D, E) HEK293T cells were transfected with UL42-Flag, A20, or vector control. Sixteen hours later, the cells were stimulated with the transfection of 500 ng/ml B-DNA and the induction of IFN-β (D) and ISG54 (E) mRNA was quantified by qPCR. (F) HEK293T cells were cotransfected with UL42-Flag or vector control and HA–IRF-3. Sixteen hours later, the cells were lysed in NP-40 lysis buffer and HA–IRF-3 was immunoprecipitated. The immunoprecipitation and input lysates were separated by SDS-PAGE and immunoblotted for UL42-Flag and HA–IRF-3. (G) HEK293T cells were cotransfected with an NF-κB–luciferase reporter, UL42-Flag, or vector control and TRAF6 or vector control. Sixteen hours after transfection, luciferase activity was measured. (H) HEK293T cells were cotransfected with an AP-1–luciferase reporter and UL42-Flag or vector control. The cells were stimulated with 2.3 nM PMA for 16 h, and luciferase activity was measured. (I) HEK293T cells were cotransfected with a cAMP-reactive element (CRE)–luciferase reporter and UL42-Flag or vector control. Sixteen hours after transfection, the cells were activated with 10 μM forskolin, and luciferase activity was measured. RLU, relative light units; IP, immunoprecipitation; HSP90, heat shock protein 90 (loading control); FSK, forskolin.

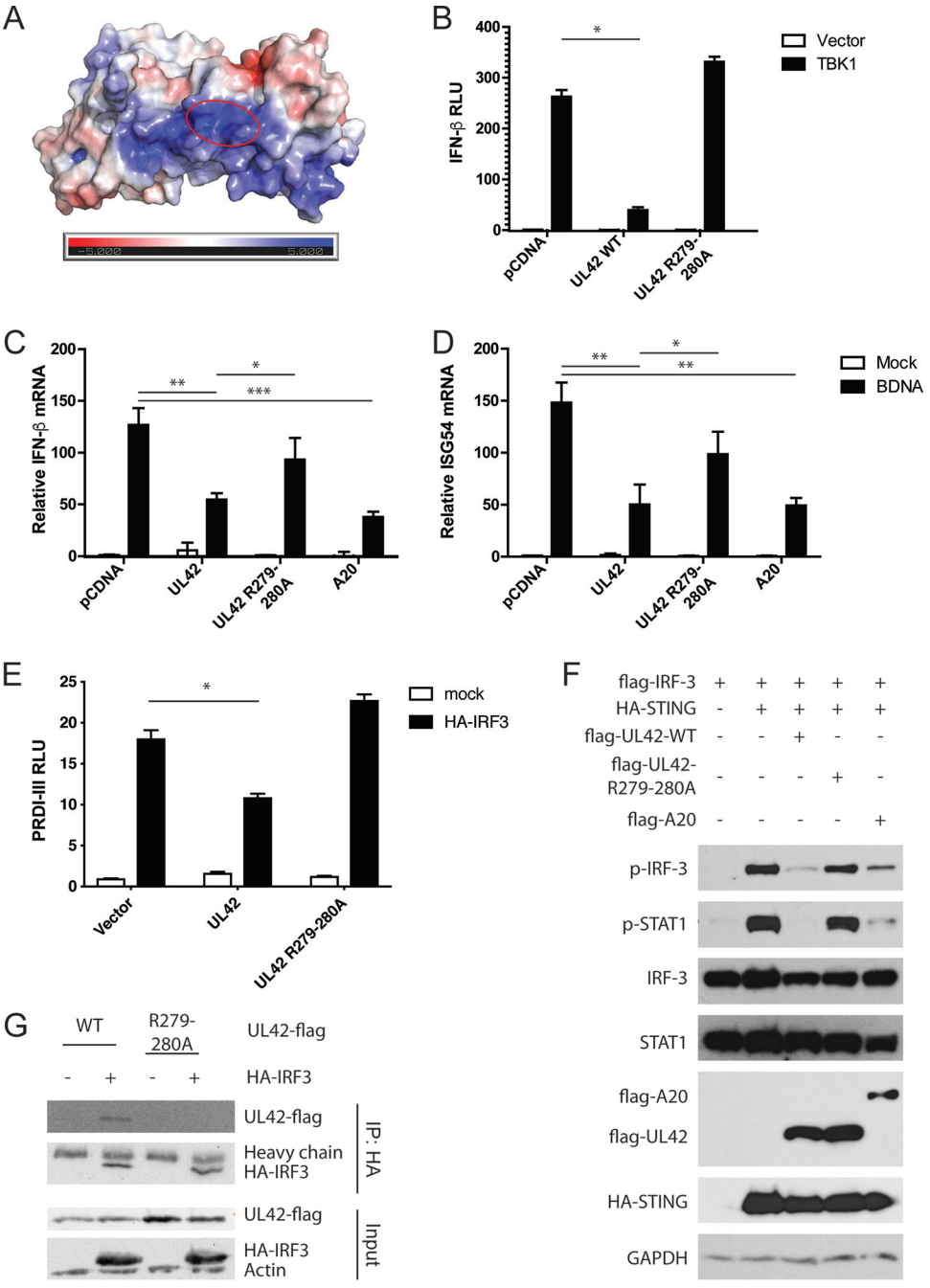

FIG 5 UL42 prevents phosphorylation of IRF-3, and mutation in the DNA-binding domain of UL42 prevents IRF-3 interaction and IFN-β inhibition. (A) DNA-binding positively charged surface of UL42 (blue). Circled are the two arginines targeted by alanine mutation; the results of experiments using the UL42 R279-280A mutant are shown in the other panels. Red-to-blue scale shows surface charge of UL42, calculated with PyMol using crystal structure from reference 29. (B) HEK293T cells were cotransfected with an IFN-β–luciferase reporter, UL42 WT, UL42 R279-280A, or vector control and TBK1. Sixteen hours after transfection, luciferase activity was measured. (C, D) IFN-β (C) and ISG54 (D) mRNA induction 24 h after 500-ng/ml B-DNA transfection in HEK293T cells expressing UL42 WT, UL42 R279-280A, A20, or pCDNA empty control. (E) HEK293T cells were cotransfected with a 4xIRF-3 PRD(I/III) reporter, UL42 WT, UL42 R279-280A, or vector control and HA–IRF-3. Sixteen hours after transfection, luciferase activity was measured. (F) HEK293T cells were cotransfected with UL42 WT, UL42 R279-280A, A20, or vector control, HA-STING or vector control, and Flag-IRF-3. Sixteen hours after transfection, the cells were lysed in NP-40 lysis buffer, and the lysates were separated on SDS-PAGE and immunoblotted for IRF-3, phospho-IRF-3 (S396), STAT1, phospho-STAT1 (Y701), Flag tag, and HA-STING. GAPDH, glyceraldehyde-3-phosphate dehydrogenase (loading control). (G) HEK293T cells were cotransfected with UL42 WT-Flag or UL42 R279-280A–Flag and HA–IRF-3 or vector control. Sixteen hours later, the cells were lysed in NP-40 lysis buffer and HA–IRF-3 was immunoprecipitated. The immunoprecipitation and input lysates were separated by SDS-PAGE and immunoblotted for UL42-Flag and HA–IRF-3. *, $P < 0.05$; **, $P < 0.01$; and ***, $P < 0.001$.

signaling (28). We therefore investigated the effect of alanine substitution at arginines 279 (R279A) and 280 (R280A) on UL42's ability to reduce IFN-β activation. Similar to previous reports, the UL42 double mutation (R279-280A) did not affect IFN-β activation in the context of TBK1 overexpression compared to the result for wild-type UL42 (Fig. 5B). Furthermore, the double mutation showed reduced inhibition of B-DNA-induced activation of IFN-β and ISG54 transcript (Fig. 5C and D). Finally, the double mutation prevented inhibition of IRF-3-driven activation of a 4xIRF3 PRD(I/III) reporter compared to the result for wild-type UL42 (Fig. 5E) (47).

A common mechanism of inhibition of transcription factor activity is to inhibit the activating phosphorylation event they undergo. To investigate whether UL42 affects IRF-3 phosphorylation, we cotransfected HEK293T cells with UL42-Flag, hemagglutinin (HA)-STING, and Flag–IRF-3 and immunoblotted for phosphorylated IRF-3. We observed that WT UL42 inhibits IRF-3 phosphorylation but the double mutant does not (Fig. 5F). This was further supported by a reduction in STAT1 phosphorylation, which is a downstream event of IFN-I expression (Fig. 5F).

While this R279-280A mutant has been described as being unable to bind DNA, we wanted to determine whether it maintained its ability to bind IRF-3. We therefore overexpressed the WT or mutant Flag-tagged UL42 with HA–IRF-3 and immunoprecipitated IRF-3. While WT UL42 is able to bind IRF-3, the mutant is not (Fig. 5G). This indicates that the double mutant loses its ability to bind IRF-3, which is consistent with the loss of activity in transcriptional regulation of IFN-β.

DISCUSSION

Numerous studies have defined the role of individual HSV-1 proteins (reviewed in reference 3) based on the construction of individual viral strains deficient in one or more viral genes. While this method has proven effective, it has multiple drawbacks, including the need to construct a mutant strain for every open reading frame, limited granularity in the analysis, and the inability to examine intergenic regions. Having limited genomes, many viruses have evolved multifunctional proteins. The major phenotype associated with knocking out such proteins can obscure their secondary functions.

To circumvent these challenges, we used an unbiased technique that has proven effective in the study of other viruses (17–19) and bacteria (20, 21) but had never been used before in HSV-1. We created a library of mutants containing a disruptive 1.2-kb insertion every 20 bp on average, with each mutant containing a single insertion. The coverage of the genome was complete, making this library an effective tool to interrogate every region of the viral genome, provided the proper selective environment exists. Interestingly, the viruses that were the fittest were those that contained insertions in some nonessential viral genes, and not intact viruses (in which the transposon did not insert in a gene related to HSV-1 biology). This seems to indicate that under these *in vitro* conditions, some genes, such as US9, are not only nonessential but actually limit the growth of the virus. Indeed, US9 has been reported to be important for anterograde transport in neural axons, which could explain why its expression is dispensable in our system (31, 32). Importantly, our strain of HSV-1 does not contain mutations preventing the expression of US9 which are present in the KOS strain (33), which would have made insertions in that ORF theoretically ineffectual.

Understanding how HSV-1 regulates the innate immune response has already aided the design of oncolytic immunotherapies (34) and could also provide insight into better antiviral therapies. By selecting our library in WT or IFNAR1$^{-/-}$ cells, we found that some previously described regulators of IFN-I were not detected in our system (UL24, UL36, VP16, UL54, and UL37). Four of these five genes were very strongly selected in WT cells, suggesting an essential function that might not be rescued in IFNAR1$^{-/-}$ cells. Surprisingly, ICP0 mutants only showed a trend toward better growth in IFNAR$^{-/-}$ cells, in spite of ICP0 having been described as targeting many pathways regulating IFN-I (4). US3, ICP34.5, and VP24 all target events that directly regulate transcription factors (24–26). These viral genes were more strongly selected than, for instance, US11, which

targets nucleic acid sensors (35). This could indicate that this screening method is more sensitive toward genes that affect molecular pathways with limited redundancy. The genes that showed the strongest differential selection—US1, UL44, and UL42—had not been described as being involved in regulating the interferon pathway before. The US1 protein of HSV-2 has been shown by Zhang et al. to inhibit type I interferon activation by blocking IRF-3 from binding to its promoter (36). In that study however, the HSV-1 US1 did not inhibit IFN-I activation. In that regard, our results are contradictory, as we were able to confirm the ability of HSV-1 US1 to block STING-induced IFN-β–luciferase reporter activation. It is possible that the viral strains our two laboratories used contain different sequences for the US1 gene that could explain this discrepancy. Despite the strong bias for growth of the mutant in IFNAR1$^{-/-}$ cells, we found that UL44 does not affect IFN-β activation. The UL44 gene encodes glycoprotein C (gC), a membrane protein important for attachment of the virion to the cell and inhibition of the C3b complement system component (37). It is important to remember that by screening in IFNAR1$^{-/-}$ cells, we are effectively looking at cells that have reduced type I interferon production, as well as reduced interferon-stimulated gene function. Interestingly, a secreted form of the protein, gCsec, has been identified, but its function has not been identified (38). Further studies could explore whether gC or gCsec has an effect on type I interferon signaling or an effect on particular ISGs.

In the context of high-throughput screening of viral mutants, one might expect genes targeting transcription factors to be more easily detected than those targeting upstream molecules. Indeed, during the infection, different pathways are engaged which converge in the activation of IFN-I. The loss of inhibition of a PRR might not be as selective for the virus as if the viral protein had targeted a transcription factor controlled by multiple PRRs. In this data set, viral proteins targeting transcription factors (US3, VP24, and ICP34.5) showed stronger selection than those targeting sensors (US11 and UL41).

We showed that UL42 is able to suppress the production of IFN-β following B-DNA stimulation or overexpression of signaling intermediates. We showed that UL42 and IRF-3 interact and that UL42 interferes with IRF-3 phosphorylation. This is surprising, considering that the IRF-3 phosphorylation event happens in the cytoplasm, while UL42 is a nuclear protein. Zhang et al. have reported that UL42 can prevent nuclear translocation of NF-κB subunits, which should also take place in the cytoplasm (28). The subcellular compartment in which the function is carried out remains to be determined, but it is possible that a minor fraction of UL42 shuttles to the cytoplasm to interact with IRF-3 and NF-κB components. Importantly, we confirmed the specificity of inhibition by showing that UL42 overexpression had no effect on the AP-1 and cAMP response element transcription pathways (Fig. 4). The fact that the double mutation R279-280A abolished DNA interaction, as well as inhibition of NF-κB and IRF-3 pathways, raises the concern that the mutant protein does not fold properly. Based on the comparable levels of protein expression between the mutant and the WT UL42 and the nuclear localization of the mutant (data not shown), we believe the protein fold is likely preserved.

The DNA polymerase processivity factor encoded by UL42 is an essential protein that, with the DNA polymerase catalytic subunit UL30, forms the viral DNA polymerase responsible for genome replication. It carries out that function by stabilizing the catalytic subunit on the DNA strand (39). Previous studies have characterized UL42 as a nuclear DNA-binding protein with no sequence specificity (40). Interestingly, early studies showed that about half of the UL42 protein was bound to UL30, while the rest was free from this complex, consistent with functions beyond DNA replication (39). Because the major function of UL42 is its role in viral genome replication, viruses in which UL42 is knocked out are nonreplicative. This prevented us from comparing the IFN activation of UL42 mutant viruses, as their wild-type counterparts replicated at a much higher rate (data not shown).

We believe that by having a relatively high multiplicity of infection (MOI) during our selection process (MOI of 0.15), as well as collecting samples after more than one

replicative cycle, there is a chance for mutants to be rescued by neighboring viruses carrying a different mutation. The main concern that arises with this possibility is whether the phenotype we observe can be attributed to a particular gene or whether it is a combinatorial phenotype from another mutant infecting the same cell. Addressing this concern highlights a strength of the high-throughput mutation strategy. Indeed, for each ORF analyzed, there exist dozens of mutants in the library. Additionally, each infection cycle was done at about 37× coverage (300,000 PFU used per biological replicate for a library of ~8,000 mutants). Therefore, we believe that the odds that a randomly occurring combinatorial phenotype will repeat over 5 passages and provide a significant effect on library selection are sufficiently low to reject this alternative hypothesis. This view is supported further by the rest of our results, which confirm that UL42 expression alone is sufficient to inhibit type I interferon activation and signaling.

To summarize, we have described a novel tool to study HSV-1 biology via screening of the entirety of its genome. We used this strategy to identify novel viral proteins that regulate the activation and signaling of type I interferon and identified the mechanism by which one of these proteins carries out that function. We believe that this strategy could be used to study the HSV-1 genome in more detail, as the granularity of the library allows analysis of sub-100-nt windows of the genome. It could also be used to better understand the role of intergenic regions. A better understanding of how HSV-1 regulates the type I interferon response provides novel antiviral targets and could improve oncolytic vector design.

MATERIALS AND METHODS

Cells and recombinant HSV-1. African green monkey kidney Vero cells and human embryonic kidney HEK293T cells were procured from ATCC. IFNAR1$^{-/-}$ A549 cells and their respective control cells were previously described (41). A bacterial artificial chromosome containing the HSV-1 genome (BAC HSV-1) was a gift of Chunfu Zheng, Fujian Medical University, Fuzhou, Fujian, China (42).

Library construction and *in vitro* passaging. A pEntranceposon-Kan vector (Thermo Fisher) was modified by PCR to insert BpuEI and KasI restriction enzyme sites at the end of the R1 site of the transposon. The transposon sequence was excised using KasI and mixed with MuA transposase (Thermo Fisher) for the transposition reaction. The transposition complex was mixed with purified BAC HSV-1, and the reaction was carried out as described by the manufacturer. The resulting DNA was electroporated into high-efficiency DH10B strain *E. coli* cells (Invitrogen), and the cells plated on chloramphenicol or chloramphenicol-kanamycin LB plates. This allowed confirmation that fewer than 70% of the BAC molecules contained a transposon insertion. Approximately 8,000 colonies with double resistance were collected, mixed, and frozen in LB with 15% glycerol. For BAC preparation, one aliquot was thawed and plated onto 10 15-cm chloramphenicol-kanamycin LB plates. The resulting lawn was collected the next day for BAC purification.

For viral preparation, 18 μg of the BAC HSV-1 library was transfected into 5 to 10 million HEK293T cells using Lipofectamine 2000 (Invitrogen). The resulting virus was used to infect 200,000,000 Vero cells at an MOI of 0.01 to prepare the input viral library.

For passaging, 1,000,000 cells were plated per well of a 6-well plate. The next day, the cells were infected for 1 h in triplicates at an MOI of 0.15 in Dulbecco modified Eagle medium (DMEM; Corning). The viral inoculum was then removed and replaced with DMEM (Corning) supplemented with 10% fetal bovine serum (FBS) and 1% penicillin-streptomycin (Gibco). Forty hours postinfection, the cells and supernatant were collected and freeze-thawed three times before being titrated by plaque assay on Vero cells. The virus collected from passage one was used to infect the cells of passage two under identical conditions. This process was repeated four times, with all replicates being passaged independently.

Library sequencing and data analysis. Infected cells and cell supernatants were collected and freeze-thawed three times. Cell lysates were cleared of cell debris by centrifugation. The virus from 500 to 1,000 μl of viral supernatant was concentrated by centrifugation at 20,200 × *g* for 90 min at 4°C. The viral particles were treated with DNase I (Sigma) at 37°C for 30 min to remove potential traces of BAC, and the viral genomes were then extracted using the PureLink viral RNA/DNA minikit (Invitrogen). Purified viral genomes were digested with BpuEI (NEB), and annealed adapter oligonucleotides were ligated overnight at 16°C using T4 ligase (NEB). The sequencing library was constructed using a two-step Nextera indexing protocol with primers specific for the transposon and the adapter oligonucleotide (Illumina). The resulting library was sequenced on a MiSeq instrument (Illumina). The adapter oligonucleotide was P-GTCGTGACTGGGAAAACCC TGGCGTTGTTGTTCGCCAGGGTTTTCCCAGTCACGACNN. The Nextera adapter primers were as follows: M13_III_F, TCGTCGGCAGCGTCAGATGTGTATAAGAGACAG(0–3N)CCAGGGTTTTCCCAGTCACG; 5p_III_R, GT CTCGTGGGCTCGGAGATGTGTATAAGAGACAG(0–3N)CAACGTGGCTTACTAGGATCCGC; and 3p_III_R, GTCT CGTGGGCTCGGAGATGTGTATAAGAGACAG(0–3N)TGTAACACTGGCAGAGCATTACGC.

Raw reads were processed by extracting the 14- to 18-nt HSV-1 sequence using cutadapt to remove the 3′ and 5′ constant sequences (43). These reads were then aligned to the reference HSV-1 genome using bowtie (44) with -m 2 --best --strata arguments. BEDTools (45) was used to extract the number of aligned reads per 100-bp window in the reference genome. The resulting counts were used as input to the TnSeqDiff (23) tool to compute fold changes and significance.

Wild-type and mutant HSV-1 gene cloning. Wild-type sequences were cloned out of the BAC HSV-1 sequence into a pCDNA3.1-Flag plasmid under the cytomegalovirus (CMV) promoter using standard techniques. Mutants were generated by PCR amplification and InFusion cloning (Clontech). All sequences were confirmed by Sanger sequencing. The primers used were as follows: US1-F, TTAATTCAGATCTAGTTCTGGAT GGCCGACATTTCC; US1-R, CCCGGGATCCTCTAGATCACGGCCGGAGAAACGTG; UL44-F, TTAATTCAGATCTAGGA GGCGTCGGGCATGGC; UL44-R, CCCGGGATCCTCTAGAGCGTTACCGCCGATGACG; UL42-F, TAGACTCGAGCGGC CGCATGACGGATTCCCCTGGCG; UL42-R, GTAATCTAGAAAGCTGGGGAATCCAAAACCAGACGG; UL42-R279-80A_F, TGCTCGCAGCGCTGCAGGTCGGCGGGGG; and UL42-R279-80A_R, TGCAGCGCTGCGAGCACCGCCC GCATGCTG.

Luciferase reporter assays. HEK293T cells were transfected with the firefly luciferase gene under the control of the IFN-β, ISRE, NF-κB, AP-1, CRE, or 4xIRF3 PRD(I/III) (a gift from S. Ludwig, Muenster University) promoter and with the *Renilla* luciferase gene under the control of the TK promoter. The cells were cotransfected with HSV-1 genes, luciferase constructs, and stimulatory genes using polyethyleneimine (PEI). Sixteen to 20 h after transfection, the cells were lysed according to the manufacturer's instructions. For stimulations, the cells were transfected with HSV-1 genes and luciferase constructs and stimulated the following day with recombinant IFN-β (Peprotek), forskolin, or PMA (Sigma) for the times indicated in the figure legends. Luciferase activities were measured using the Dual-Luciferase reporter assay system (Promega). The firefly luciferase signal was normalized to the *Renilla* luciferase signal for analysis.

Real-time PCR. HEK293T cells were transfected with HSV-1 proteins using PEI (Polysciences). The next day, cells were stimulated with 500 ng/ml B-DNA (InvivoGen) using Lipofectamine 2000 (Invitrogen). Zero to 24 h later, total RNA was collected and later extracted using TRIzol reagent (Invitrogen). Identical amounts of total RNA from each sample were reverse transcribed using iScript (Bio-Rad). Relative expression was measured using iTaq (Bio-Rad) quantitative PCR (qPCR) reagent and calculated using PSMB2 as a housekeeping gene reference. The primers used were as follows: PSMB2-F, ATCCTCGACCG ATACTACACAC; PSMB2-R, GAACACTGAAGGTTGGCAGAT; hIFNb-F, TGTGGCAATTGAATGGGAGGCTTGA; hIFNb-R, CGGCGTCCTCCTTCTGGAACT; hISG54-F, TGCAACCTACTGGCCTATCTA; and hISG54-R, CAGGTGA CCAGACTTCTGATT.

Immunoprecipitation and immunoblotting. HEK293T cells were cotransfected with UL42-Flag (WT or R279-280A mutant) and HA–IRF-3. Sixteen to 24 h later, cells were lysed in NP-40 lysis buffer (50 mM Tris-Cl, pH 7.4, 150 mM NaCl, 1 mM EDTA, 1% NP-40) supplemented with complete protease inhibitors (Roche) and HA–IRF-3 was pulled down using a rabbit anti-HA antibody (sc-805; Santa Cruz) and protein A magnetic beads (Bio-Rad). The beads were washed 3 times according to the manufacturer's instructions, and the immunoprecipitated and input fractions were separated via SDS-PAGE. Proteins were transferred onto polyvinylidene difluoride (PVDF) membranes and probed for Flag (F1804; Sigma), HA (sc-805; Santa Cruz), and β-actin (Cell Signaling).

HEK293T cells were cotransfected with UL42-Flag (WT or R279-280A mutant), HA-STING, and Flag-IRF-3. Sixteen to 24 h later, cells were lysed in NP-40 lysis buffer (50 mM Tris-Cl, pH 7.4, 150 mM NaCl, 1 mM EDTA, 1% NP-40) supplemented with complete protease inhibitors (Roche) and lysates were separated via SDS-PAGE. Proteins were transferred to PVDF membranes and immunoblotted with antibodies against IRF-3 (Cell Signaling), p-IRF-3 S396 (Cell Signaling), STAT1 (Santa Cruz Biotechnology), p-STAT1 Y701 (Cell Signaling), HA (sc-805; Santa Cruz), and Flag (F1804; Sigma).

Statistical analysis. Data are presented as mean values $\pm$ standard deviations and are representative of at least two experiments. Statistical significance was calculated using the Student *t* test in GraphPad Prism 5.04 software.

Data availability. The HSV-1 BAC wild-type reference sequence used to align our library is available in GenBank under accession number MN458559.

ACKNOWLEDGMENTS

We thank Chunfu Zheng for the HSV-1 BAC construct. We thank Stephan Ludwig for providing us with the 4xIRF3 PRD(I/III) luciferase reporter construct. We thank Charles Hwang for providing us with the HSV-1 UL42 mutant virus and associated V9 Vero cell line. We thank Serghei Mangul for technical assistance and Andrew Ah Young and Sarah Christofersen for critical reviews of the manuscript.

M.C. was supported by the Whitcome Fellowship Program. This work was supported by NIH grant number R01 AI069120.

REFERENCES

1. Smith JS, Robinson NJ. 2002. Age-specific prevalence of infection with herpes simplex virus types 2 and 1: a global review. J Infect Dis 186(Suppl 1):S3–28. https://doi.org/10.1086/343739.
2. Koyuncu OO, Hogue IB, Enquist LW. 2013. Virus infections in the nervous system. Cell Host Microbe 13:379–393. https://doi.org/10.1016/j.chom.2013.03.010.
3. Everett RD. 2014. HSV-1 biology and life cycle. Methods Mol Biol 1144:1–17. https://doi.org/10.1007/978-1-4939-0428-0_1.
4. Su C, Zhan G, Zheng C. 2016. Evasion of host antiviral innate immunity by HSV-1, an update. Virol J 13:38. https://doi.org/10.1186/s12985-016-0495-5.
5. Zheng C. 2018. Evasion of cytosolic DNA-stimulated innate immune responses by herpes simplex virus 1. J Virol 92:e00099-17. https://doi.org/10.1128/JVI.00099-17.
6. McNab F, Mayer-Barber K, Sher A, Wack A, O'Garra A. 2015. Type I interferons in infectious disease. Nat Rev Immunol 15:87–103. https://doi.org/10.1038/nri3787.
7. Akira S, Uematsu S, Takeuchi O. 2006. Pathogen recognition and innate immunity. Cell 124:783–801. https://doi.org/10.1016/j.cell.2006.02.015.
8. Sun L, Wu J, Du F, Chen X, Chen ZJ. 2013. Cyclic GMP-AMP synthase is a cytosolic DNA sensor that activates the type I interferon pathway. Science 339:786–791. https://doi.org/10.1126/science.1232458.

9. Zhang X, Wu J, Du F, Xu H, Sun L, Chen Z, Brautigam CA, Zhang X, Chen ZJ. 2014. The cytosolic DNA sensor cGAS forms an oligomeric complex with DNA and undergoes switch-like conformational changes in the activation loop. Cell Rep 6:421–430. https://doi.org/10.1016/j.celrep.2014.01.003.
10. Tanaka Y, Chen ZJ. 2012. STING specifies IRF3 phosphorylation by TBK1 in the cytosolic DNA signaling pathway. Sci Signal 5:ra20. https://doi.org/10.1126/scisignal.2002521.
11. Devasthanam AS. 2014. Mechanisms underlying the inhibition of interferon signaling by viruses. Virulence 5:270–277. https://doi.org/10.4161/viru.27902.
12. Taylor KE, Mossman KL. 2013. Recent advances in understanding viral evasion of type I interferon. Immunology 138:190–197. https://doi.org/10.1111/imm.12038.
13. Su C, Zheng C. 2017. Herpes simplex virus 1 abrogates the cGAS/STING-mediated cytosolic DNA-sensing pathway via its virion host shutoff protein, UL41. J Virol 91:e02414-16. https://doi.org/10.1128/JVI.02414-16.
14. Christensen MH, Jensen SB, Miettinen JJ, Luecke S, Prabakaran T, Reinert LS, Mettenleiter T, Chen ZJ, Knipe DM, Sandri-Goldin RM, Enquist LW, Hartmann R, Mogensen TH, Rice SA, Nyman TA, Matikainen S, Paludan SR. 2016. HSV-1 ICP27 targets the TBK1-activated STING signalsome to inhibit virus-induced type I IFN expression. EMBO J 35:1385–1399. https://doi.org/10.15252/embj.201593458.
15. Lin R, Noyce RS, Collins SE, Everett RD, Mossman KL. 2004. The herpes simplex virus ICP0 RING finger domain inhibits IRF3- and IRF7-mediated activation of interferon-stimulated genes. J Virol 78:1675–1684. https://doi.org/10.1128/jvi.78.4.1675-1684.2004.
16. Deschamps T, Kalamvoki M. 2017. Evasion of the STING DNA-sensing pathway by VP11/12 of herpes simplex virus 1. J Virol 91:e00535-17. https://doi.org/10.1128/JVI.00535-17.
17. Zhan X, Lee M, Abenes G, Von Reis I, Kittinunvorakoon C, Ross-Macdonald P, Snyder M, Liu F. 2000. Mutagenesis of murine cytomegalovirus using a Tn3-based transposon. Virology 266:264–274. https://doi.org/10.1006/viro.1999.0089.
18. Song MJ, Hwang S, Wong WH, Wu T-T, Lee S, Liao H-I, Sun R. 2005. Identification of viral genes essential for replication of murine gamma-herpesvirus 68 using signature-tagged mutagenesis. Proc Natl Acad Sci U S A 102:3805–3810. https://doi.org/10.1073/pnas.0404521102.
19. Wang L, Liu S-Y, Chen H-W, Xu J, Chapon M, Zhang T, Zhou F, Wang YE, Quanquin N, Wang G, Tian X, He Z, Liu L, Yu W, Sanchez DJ, Liang Y, Jiang T, Modlin R, Bloom BR, Li Q, Deng JC, Zhou P, Qin F-F, Cheng G. 2017. Generation of a live attenuated influenza vaccine that elicits broad protection in mice and ferrets. Cell Host Microbe 21:334–343. https://doi.org/10.1016/j.chom.2017.02.007.
20. Hensel M, Shea JE, Gleeson C, Jones MD, Dalton E, Holden DW. 1995. Simultaneous identification of bacterial virulence genes by negative selection. Science 269:400–403. https://doi.org/10.1126/science.7618105.
21. van Opijnen T, Bodi KL, Camilli A. 2009. Tn-seq: high-throughput parallel sequencing for fitness and genetic interaction studies in microorganisms. Nat Methods 6:767–772. https://doi.org/10.1038/nmeth.1377.
22. Polvino-Bodnar M, Orberg PK, Schaffer PA. 1987. Herpes simplex virus type 1 oriL is not required for virus replication or for the establishment and reactivation of latent infection in mice. J Virol 61:3528–3535.
23. Zhao L, Anderson MT, Wu W, T Mobley HL, Bachman MA. 2017. TnseqDiff: identification of conditionally essential genes in transposon sequencing studies. BMC Bioinformatics 18:326. https://doi.org/10.1186/s12859-017-1745-2.
24. Wang S, Wang K, Lin R, Zheng C. 2013. Herpes simplex virus 1 serine/threonine kinase US3 hyperphosphorylates IRF3 and inhibits beta interferon production. J Virol 87:12814–12827. https://doi.org/10.1128/JVI.02355-13.
25. Zhang D, Su C, Zheng C. 2016. Herpes simplex virus 1 serine protease VP24 blocks the DNA-sensing signal pathway by abrogating activation of interferon regulatory factor 3. J Virol 90:5824–5829. https://doi.org/10.1128/JVI.00186-16.
26. Verpooten D, Ma Y, Hou S, Yan Z, He B. 2009. Control of TANK-binding kinase 1-mediated signaling by the γ134.5 protein of herpes simplex virus 1. J Biol Chem 284:1097–1105. https://doi.org/10.1074/jbc.M805905200.
27. Parvatiyar K, Barber GN, Harhaj EW. 2010. TAX1BP1 and A20 inhibit antiviral signaling by targeting TBK1-IKKi kinases. J Biol Chem 285:14999–15009. https://doi.org/10.1074/jbc.M110.109819.
28. Zhang J, Wang S, Wang K, Zheng C. 2013. Herpes simplex virus 1 DNA polymerase processivity factor UL42 inhibits TNF-α-induced NF-κB activation by interacting with p65/RelA and p50/NF-κB1. Med Microbiol Immunol 202:313–325. https://doi.org/10.1007/s00430-013-0295-0.
29. Zuccola HJ, Filman DJ, Coen DM, Hogle JM. 2000. The crystal structure of an unusual processivity factor, herpes simplex virus UL42, bound to the C terminus of its cognate polymerase. Mol Cell 5:267–278. https://doi.org/10.1016/S1097-2765(00)80422-0.
30. Randell JCW, Komazin G, Jiang C, Hwang CBC, Coen DM. 2005. Effects of substitutions of arginine residues on the basic surface of herpes simplex virus UL42 support a role for DNA binding in processive DNA synthesis. J Virol 79:12025–12034. https://doi.org/10.1128/JVI.79.18.12025-12034.2005.
31. Tomishima MJ, Enquist LW. 2001. A conserved alpha-herpesvirus protein necessary for axonal localization of viral membrane proteins. J Cell Biol 154:741–752. https://doi.org/10.1083/jcb.200011146.
32. Polcicova K, Biswas PS, Banerjee K, Wisner TW, Rouse BT, Johnson DC. 2005. Herpes keratitis in the absence of anterograde transport of virus from sensory ganglia to the cornea. Proc Natl Acad Sci U S A 102:11462–11467. https://doi.org/10.1073/pnas.0503230102.
33. Negatsch A, Mettenleiter TC, Fuchs W. 2011. Herpes simplex virus type 1 strain KOS carries a defective US9 and a mutated US8A gene. J Gen Virol 92:167–172. https://doi.org/10.1099/vir.0.026484-0.
34. Liu BL, Robinson M, Han Z-Q, Branston RH, English C, Reay P, McGrath Y, Thomas SK, Thornton M, Bullock P, Love CA, Coffin RS. 2003. ICP34.5 deleted herpes simplex virus with enhanced oncolytic, immune stimulating, and anti-tumour properties. Gene Ther 10:292–303. https://doi.org/10.1038/sj.gt.3301885.
35. Xing J, Wang S, Lin R, Mossman KL, Zheng C. 2012. Herpes simplex virus 1 tegument protein US11 downmodulates the RLR signaling pathway via direct interaction with RIG-I and MDA-5. J Virol 86:3528–3540. https://doi.org/10.1128/JVI.06713-11.
36. Zhang M, Liu Y, Wang P, Guan X, He S, Luo S, Li C, Hu K, Jin W, Du T, Yan Y, Zhang Z, Zheng Z, Wang H, Hu Q. 2015. HSV-2 immediate-early protein US1 inhibits IFN-β production by suppressing association of IRF-3 with IFN-β promoter. J Immunol 194:3102–3115. https://doi.org/10.4049/jimmunol.1401538.
37. Spear PG. 2004. Herpes simplex virus: receptors and ligands for cell entry. Cell Microbiol 6:401–410. https://doi.org/10.1111/j.1462-5822.2004.00389.x.
38. Sedlackova L, Perkins KD, Lengyel J, Strain AK, van Santen VL, Rice SA. 2008. Herpes simplex virus type 1 ICP27 regulates expression of a variant, secreted form of glycoprotein C by an intron retention mechanism. J Virol 82:7443–7455. https://doi.org/10.1128/JVI.00388-08.
39. Gottlieb J, Marcy AI, Coen DM, Challberg MD. 1990. The herpes simplex virus type 1 UL42 gene product: a subunit of DNA polymerase that functions to increase processivity. J Virol 64:5976–5987.
40. Randell JC, Coen DM. 2001. Linear diffusion on DNA despite high-affinity binding by a DNA polymerase processivity factor. Mol Cell 8:911–920. https://doi.org/10.1016/S1097-2765(01)00355-0.
41. Li C, Deng Y-Q, Wang S, Ma F, Aliyari R, Huang X-Y, Zhang N-N, Watanabe M, Dong H-L, Liu P, Li X-F, Ye Q, Tian M, Hong S, Fan J, Zhao H, Li L, Vishlaghi N, Buth JE, Au C, Liu Y, Lu N, Du P, Qin F-F, Zhang B, Gong D, Dai X, Sun R, Novitch BG, Xu Z, Qin C-F, Cheng G. 2017. 25-Hydroxycholesterol protects host against Zika virus infection and its associated microcephaly in a mouse model. Immunity 46:446–456. https://doi.org/10.1016/j.immuni.2017.02.012.
42. Li Y, Wang S, Zhu H, Zheng C. 2011. Cloning of the herpes simplex virus type 1 genome as a novel luciferase-tagged infectious bacterial artificial chromosome. Arch Virol 156:2267–2272. https://doi.org/10.1007/s00705-011-1094-9.
43. Martin M. 2011. Cutadapt removes adapter sequences from high-throughput sequencing reads. Embnet J 17:10–12. https://doi.org/10.14806/ej.17.1.200.
44. Langmead B, Trapnell C, Pop M, Salzberg SL. 2009. Ultrafast and memory-efficient alignment of short DNA sequences to the human genome. Genome Biol 10:R25. https://doi.org/10.1186/gb-2009-10-3-r25.
45. Quinlan AR, Hall IM. 2010. BEDTools: a flexible suite of utilities for comparing genomic features. Bioinformatics 26:841–842. https://doi.org/10.1093/bioinformatics/btq033.
46. Manservigi R, Argnani R, Marconi P. 2010. HSV recombinant vectors for gene therapy. Open Virol J 4:123–156. https://doi.org/10.2174/1874357901004030123.
47. Ehrhardt C, Kardinal C, Wurzer WJ, Wolff T, von Eichel-Streiber C, Pleschka S, Planz O, Ludwig S. 2004. Rac1 and PAK1 are upstream of IKK-ε and TBK-1 in the viral activation of interferon regulatory factor-3. FEBS Lett 567:230–238. https://doi.org/10.1016/j.febslet.2004.04.069.